

Removal of Cd²⁺ from Water Containing Ca²⁺, Mg²⁺ using Titanate Nanotubes Modified by Carbon

Mingda Wu

Nanjing Tech University

Linghong Lu (✉ linghonglu@njtech.edu.cn)

Nanjing Tech University

Tao Zhou

Nanjing Tech University

Yi Ma

Nanjing Tech University

Zhengsong Weng

Nanjing Tech University

Research Article

Keywords: Water treatment, Cadmium ion, Titanate nanotubes, carbon-modification

Posted Date: October 29th, 2021

DOI: <https://doi.org/10.21203/rs.3.rs-991276/v1>

License:  This work is licensed under a Creative Commons Attribution 4.0 International License.

[Read Full License](#)

Version of Record: A version of this preprint was published at Environmental Science and Pollution Research on February 9th, 2022. See the published version at <https://doi.org/10.1007/s11356-022-19002-7>.

2.1 Materials and reagents

TiO₂ (anatase, 2-5 nm, 98%)

Cadmium standard solution (1000 ug/mL in 1 mol/L HCl) were purchased from Shanghai Aladdin Biochemical Technology Co., Ltd. Furfuryl alcohol (>99%), Ethanol, Calcium chloride anhydrous (CaCl₂, >99%) and Cadmium nitrate tetrahydrate (>99%) were obtained from Sinopharm Chemical Reagent Co., Ltd (Shanghai, China). Magnesium chloride hexahydrate (MgCl₂·6H₂O) and Sodium hydroxide (NaOH, >99%) were both acquired from XiLong Scientific Co., Ltd (Guangdong, China).

2.2 Preparation of TNT, TNT/C and TNT/HC

2.2.1 Preparation of TNT

Mix 1.2 g of TiO₂ with 60 mL of 10 M NaOH solution. After stirring overnight, the mixture was poured into a container lined with polytetrafluoroethylene, and then heated at 130°C for 3 days.

Until the temperature of the mixed solution was consistent with room temperature, rinsed the sample with pure water until the supernatant reached neutrality. Then the target product was sonicated in alcohol and lastly dried at 80°C (Li et al. 2015).

2.2.2 Preparation of TiO₂/C and

TNT/C

3 g TiO_2 and 1 g Furfuryl alcohol were mixed with 10 mL Ethanol. After stirring for 12 hours, the furfuryl alcohol in the mixed suspension was polymerized at 80°C , and then calcined at 600°C for 3 hours under a nitrogen atmosphere. This was how TiO_2/C was made. The making process of TNT/C was the same as that of TNTs, except that the TiO_2 was replaced with TiO_2/C .

2.2.3 Preparation of TiO_2/HC and TNT/HC

Treat TiO_2/C in boiling HNO_3 for 6 hours. After standing, the supernatant was poured out, washed with deionized water to neutrality, and dried at 105°C to obtain a TiO_2/HC sample (Maroto-Valer et al. 2004). The making process of TNT/HC was the same as that of TNT, except that the TiO_2 was replaced with TiO_2/HC .

The synthesis process of the adsorbent is shown in figure 1.

2.3 Characterization of adsorbent

The morphology of these adsorbents was observed by SEM (Tescan, A VEGA) and TEM (JEM-2100Plus). The structures of these three samples were studied by XRD (Panalytical X'Pert PRO MPD). The carbon

43 content of the composite material was determined from TGA
44 (NETZSCH STA 409 PC/PG). FT-IR (TENSOR 27,
45 resolution 4 cm^{−1}, Bruker, Billerica, MA, USA)
46 was used to analyze the functional groups and bonding conditions on
47 the surface of the adsorption material. XPS (K-ALPHA, Thermo
48 Fisher, Waltham, MA, USA) was used to analyze the surface
49 element composition and valence state of the surface. The
50 concentration of Cd²⁺ was detected by A flame atomic
51 absorption spectrophotometer (FLAAS) (AA900T, PerkinElmer,
52 Waltham, MA, USA).

53 <p>2.4 Adsorption experiments</p>

54 <p>All batch experiments were repeated 3 times and oscillated at a
55 speed of 200 rpm at the set temperature. The general experimental
56 procedure is described as follows: All batch experiments were
57 carried out by adding 0.02g adsorbent to polyethylene pipe (50 ml)
58 with 40 ml solutions. When Initial solution concentration is 200
59 mg/L with the pH from 2 to 6, the most suitable pH for the
60 adsorption of Cd²⁺ by TNT, TNT/C, and TNT/HC is
61 first determined. At 25°C and the optimum pH, the adsorption
62 isotherm is obtained by experimenting with initial solutions of
63 different concentrations. At the same time, the adsorption kinetic

64 data was obtained by testing the adsorption capacity under different
65 contact time intervals.</p>

66 <p>After the set adsorption time is reached, the supernatant obtained
67 after filtering the aqueous suspension through a 0.45um filter
68 membrane can be used for the measurement of Cd²⁺
69 concentration. </p>

70 <p>The data is the average of three experiments. The adsorption
71 capacity q_e (mg/g) was calculated by the eq. (1) (Zhu et al.
72 2018)</p>

73 <p></p>

76 <p>Where c_0 (mg/L) is the concentration of initial Cd²⁺
77 concentration and C_e (mg/L) is the equilibrium Cd²⁺ concentration,
78 respectively, V (L) is the volume of the solution and m (g) is the
79 weight of sorbent.</p>Removal of Cd²⁺ from water containing Ca²⁺,
80 Mg²⁺ using Titanate nanotubes modified by carbon

81 *Mingda Wu, Linghong Lu**, Tao Zhou, Yi Ma, Zhongsong Weng

82 College of Chemical Engineering, State Key Laboratory of Materials-oriented
83 Chemical Engineering, Nanjing Tech University, Nanjing 211816, P.R. China

* Corresponding Author E-mail: linghonglu@njtech.edu.cn (L.H. Lu)

84 Abstract

85 Ca^{2+} and Mg^{2+} usually exist in natural water. When Cd^{2+} is removed from water
86 by adsorption, it will be inhibited by these two ions. Titanate nanotubes (TNTs) have
87 an effective adsorption capacity for Cd^{2+} due to extraordinary ion-exchange property.
88 However, TNTs also adsorb Ca^{2+} and Mg^{2+} in water. In this study, carbon-modified TNT
89 (TNT/C or TNT/HC) was synthesized by hydrothermal synthesis. The transmission
90 electron microscope (TEM) images show that TNT/C or TNT/HC still keep nanotube
91 morphology. The experimental results show the order of adsorption amount to Cd^{2+} is
92 $\text{TNT} > \text{TNT/C} > \text{TNT/HC}$ when there is no Ca^{2+} or Mg^{2+} . But when there is Ca^{2+} or
93 Mg^{2+} in the water, the order of Cd^{2+} adsorption capacity becomes $\text{TNT/HC} > \text{TNT/C} >$
94 TNT . It indicates that the surface carbon-modification can alleviate the hindrance of
95 Ca^{2+} or Mg^{2+} to Cd^{2+} removal. This is because the carbon on the surface of TNT
96 captured part of Ca^{2+} or Mg^{2+} , it made more Cd^{2+} be successfully absorbed by TNT
97 through ion exchange. This mechanism was confirmed by XPS spectra analysis. The
98 results of this paper can provide ideas for the adsorption and removal of Cd^{2+} in water
99 in the presence of Ca^{2+} or Mg^{2+} .

100 Keywords

101 Water treatment; Cadmium ion; Titanate nanotubes; carbon-modification

102 1. Introduction

103 With the increase of cadmium production year by year, a considerable amount of
104 cadmium is discharged into the environment, and many natural water systems are
105 polluted by cadmium (Zhao et al. 2011). Unreasonable disposal of heavy metal-
106 containing wastewater poses a huge threat to human health (Zhou et al. 2018).
107 Cadmium ion (Cd^{2+}) is one of the toxic ions, and the In the World Health
108 Organization's regulations on qualified drinking water, the maximum concentration of
109 Cd^{2+} is limited to 5 $\mu\text{g/L}$ (Sriram et al. 2020). The effects of intaking the drinking water
110 whose Cd^{2+} concentration exceeds the limit ingestion are inducing kidney disease and

111 bone disease (Zhang et al. 2019). The Japanese “itai-itai” disease is the worst event in
112 the Cd²⁺ pollution incident, and it is included in the eight major pollution
113 incidents(Huang et al. 2020a).

114 There are many methods to treat water with heavy metal ions, including physical
115 methods, chemical methods, membrane treatment methods, and electrolysis methods
116 (Bolisetty et al. 2019). Among them, the adsorption method has become one of the most
117 promising methods for the treatment of metal ions due to its low cost, simple operation
118 process, and less post-treatment (Mudhoo et al. 2020). However, traditional adsorbents,
119 such as carbon-based adsorbents and organic polymer adsorbents, do not have a good
120 adsorption capability on Cd²⁺ (Lu &Astruc 2018). In contrast, nano-metal oxide
121 materials have shown potential applications in anchoring Cd²⁺. Among them,
122 magnesium oxide, iron oxide, manganese oxide, and aluminum oxide have all been
123 used as adsorbents for heavy metal ions (Boparai et al. 2011, Mahdavi et al. 2013, Yusuf
124 et al. 2020, Zhang et al. 2020). However, due to the instability of these substances in
125 water, these oxides are not enough to be perfect Cd²⁺ adsorbent materials. Titanate
126 nanotubes have attracted the attention of researchers since it successfully prepared by
127 Tomoko Kasuga in 1998 (Kasuga et al. 1998), it has received extensive attention from
128 researchers due to their excellent specific surface area, excellent hydrophilicity and
129 stability in complex water environments. This material is generally obtained by one-
130 step hydrothermal treatment of titanium dioxide in a high-concentration NaOH aqueous
131 solution at medium temperature (90-180°C), and could be obtained from various crystal
132 forms of titanium oxide raw materials (Bi et al. 2020). Allen J. Du et al. found that when
133 there are both inner sphere complexation and ion exchange, the multi-site ion
134 complexation (CDMUSIC) model based on charge distribution is the most consistent
135 with the process of TNT adsorption of Cd²⁺ (Du et al. 2011). Xiong et al. found that
136 with the pH of the initial solution changed from 2 to 6, the ability of Cd²⁺ adsorbed by
137 TNT was increased (Xiong et al. 2011). In addition, it was confirmed that 0.1 M
138 hydrochloric acid can desorb 85% of Cd²⁺ from the adsorbent (Xiong et al. 2011). Liu

139 et al. found that Na^+ , K^+ , Ca^{2+} and Mg^{2+} will compete with Cd^{2+} , which greatly inhibited
140 the adsorption of Cd^{2+} (Liu et al. 2013). Moreover, it is proposed that EDTA and HNO_3
141 can also be used as desorption agents to desorb Cd^{2+} from TNT, and the desorption rate
142 can reach more than 90% (Liu et al. 2013). Moreover, it was proved that the $[\text{TiO}_6]$
143 octahedral structure of TNTs hardly changed during the entire adsorption process (Duan
144 et al. 2021). This shows that TNT has high structural stability when facing the complex
145 environment of the waste water (Wang et al. 2013a). Wang et al. used 0.1 M HNO_3 to
146 desorb the Cd^{2+} in TNT, and then only 0.2 M NaOH at room temperature could easily
147 achieve the regeneration of TNT. Even after six cycles, the regenerated TNT can adsorb
148 Cd^{2+} (Wang et al. 2013b). The research results show low NaOH concentration is
149 required to prepare TNT with the largest adsorption capacity for Cd^{2+} (Liu et al. 2014).
150 Yang et al. successfully prepared a magnetite-graphene oxide-titanate composite
151 material, which made the titanate material easier to recycle. (Yang et al. 2020).

152 Although titanate materials (TNT or TNs) have great potential as cadmium ion
153 adsorbents, when it is surrounded by Na^+ , K^+ , Ca^{2+} , Mg^{2+} and natural organic matter
154 (NOM), the adsorption capacity of Cd^{2+} would be greatly reduced. The powdered
155 activated carbon supported TNTs (TNTs@PAC) synthesized by Ma et al. showed high
156 adsorption capacity for Pb(II) and strong resistance to natural organic matter (Ma et al.
157 2017). This shows that the researchers found that the environment affects the adsorption
158 of titanate. However, few researchers are interested in the effect of inorganic ions on
159 the adsorption of titanate. Ca^{2+} and Mg^{2+} often appear in polluted water bodies, they
160 would reduce the adsorption capacity of titanate materials for Cd^{2+} : from 2.02 mmol/g
161 to 1.17 mmol/g (Liu et al. 2013). According to the soft and hard acid-base theory,
162 Ca^{2+} and Mg^{2+} belong to the ranks of hard acid, while Cd^{2+} is classified as soft
163 acid (Esrafilı et al. 2021, Wang et al. 2019). In addition, some carbon-containing
164 functional groups, such as $-\text{COOH}$, $-\text{C}=\text{O}$ and $\text{C}-\text{OH}$, are in the category of hard bases
165 (Di Natale et al. 2020, Zhao et al. 2011). If the surface of the Titanate material is
166 functionalized with $-\text{COOH}$, $-\text{C}=\text{O}$ and $-\text{OH}$, they would be used to capture Ca^{2+} , Mg^{2+} ,

167 and the probability of ion exchange between these interfering ions and the sodium ions
168 in the titanate layer would be reduced. It is beneficial to the adsorption of Cd^{2+} .

169 Based on the above statement, after carbonizing the furfuryl alcohol on the surface
170 of the titanium oxide, it was further processed by alkaline hydrothermal method to
171 obtain in-situ carbon-supported TNT.

172 This article aims to:

- 173 1) Synthesis of Titanate nanotubes modified by carbon (TNT/C);
- 174 2) Evaluate the selective adsorption performance of TNT/C;
- 175 3) Explore the mechanism of resisting interference from non-target ions by oxidizing
176 surface carbon with nitric acid.

177

178 2. Experimental

179 2.1 Materials and reagents

180 TiO_2 (anatase, 2-5 nm, 98%) and Cadmium standard solution (1000 $\mu\text{g}/\text{mL}$ in 1 mol/L
181 HCl) were purchased from Shanghai Aladdin Biochemical Technology Co., Ltd.
182 Furfuryl alcohol (>99%), Ethanol, Calcium chloride anhydrous (CaCl_2 , >99%) and
183 Cadmium nitrate tetrahydrate (>99%) were obtained from Sinopharm Chemical
184 Reagent Co., Ltd (Shanghai, China). Magnesium chloride hexahydrate ($\text{MgCl}_2 \cdot 6\text{H}_2\text{O}$)
185 and Sodium hydroxide (NaOH, >99%) were both acquired from XiLong Scientific Co.,
186 Ltd (Guangdong, China).

187

188 2.2 Preparation of TNT, TNT/C and TNT/HC

189 2.2.1 Preparation of TNT

190 Mix 1.2 g of TiO_2 with 60 mL of 10 M NaOH solution. After stirring overnight,
191 the mixture was poured into a container lined with polytetrafluoroethylene, and then
192 heated at 130°C for 3 days. Until the temperature of the mixed solution was consistent
193 with room temperature, rinsed the sample with pure water until the supernatant reached
194 neutrality. Then the target product was sonicated in alcohol and lastly dried at 80°C (Li

195 et al. 2015).

196

197 2.2.2 Preparation of TiO₂/C and TNT/C

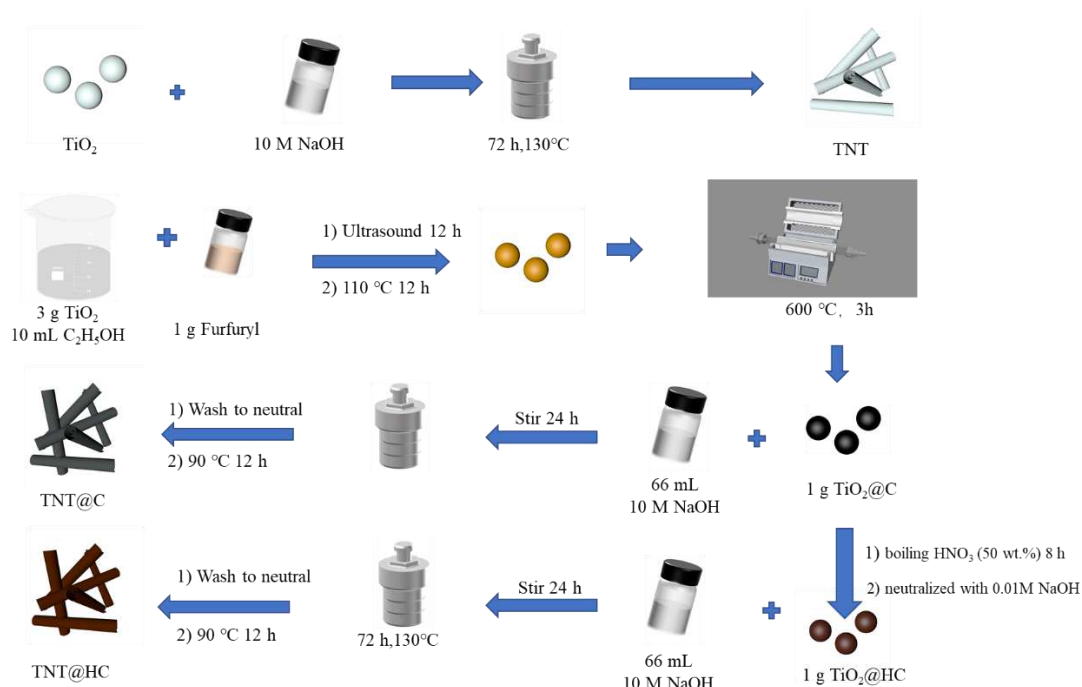
198 3 g TiO₂ and 1 g Furfuryl alcohol were mixed with 10 mL Ethanol. After stirring
199 for 12 hours, the furfuryl alcohol in the mixed suspension was polymerized at 80°C,
200 and then calcined at 600°C for 3 hours under a nitrogen atmosphere. This was how
201 TiO₂/C was made. The making process of TNT/C was the same as that of TNTs, except
202 that the TiO₂ was replaced with TiO₂/C.

203

204 2.2.3 Preparation of TiO₂/HC and TNT/HC

205 Treat TiO₂/C in boiling HNO₃ for 6 hours. After standing, the supernatant was
206 poured out, washed with deionized water to neutrality, and dried at 105°C to obtain a
207 TiO₂/HC sample (Maroto-Valer et al. 2004). The making process of TNT/HC was the
208 same as that of TNT, except that the TiO₂ was replaced with TiO₂/HC.

209 The synthesis process of the adsorbent is shown in figure 1.



210

211

Fig. 1. The scheme of the synthesis of TNT, TNT/C and TNT/HC.

212

213 2.3 Characterization of adsorbent

214 The morphology of these adsorbents was observed by SEM (Tescan, A VEGA)
215 and TEM (JEM-2100Plus). The structures of these three samples were studied by XRD
216 (Panalytical X'Pert PRO MPD). The carbon content of the composite material was
217 determined from TGA (NETZSCH STA 409 PC/PG). FT-IR (TENSOR 27, resolution
218 4 cm^{-1} , Bruker, Billerica, MA, USA) was used to analyze the functional groups and
219 bonding conditions on the surface of the adsorption material. XPS (K-ALPHA, Thermo
220 Fisher, Waltham, MA, USA) was used to analyze the surface element composition and
221 valence state of the surface. The concentration of Cd^{2+} was detected by A flame atomic
222 absorption spectrophotometer (FLAAS) (AA900T, PerkinElmer, Waltham, MA, USA).

223

224 2.4 Adsorption experiments

225 All batch experiments were repeated 3 times and oscillated at a speed of 200 rpm
226 at the set temperature. The general experimental procedure is described as follows: All
227 batch experiments were carried out by adding 0.02g adsorbent to polyethylene pipe (50
228 ml) with 40 ml solutions. When Initial solution concentration is 200 mg/L with the pH
229 from 2 to 6, the most suitable pH for the adsorption of Cd^{2+} by TNT, TNT/C, and
230 TNT/HC is first determined. At 25°C and the optimum pH, the adsorption isotherm is
231 obtained by experimenting with initial solutions of different concentrations. At the same
232 time, the adsorption kinetic data was obtained by testing the adsorption capacity under
233 different contact time intervals.

234 After the set adsorption time is reached, the supernatant obtained after filtering the
235 aqueous suspension through a 0.45um filter membrane can be used for the measurement
236 of Cd^{2+} concentration.

237 The data is the average of three experiments. The adsorption capacity q_e (mg/g)
238 was calculated by the Eq. (1) (Zhu et al. 2018)

$$239 q_e = (c_0 - c_e) * V/m \quad (1)$$

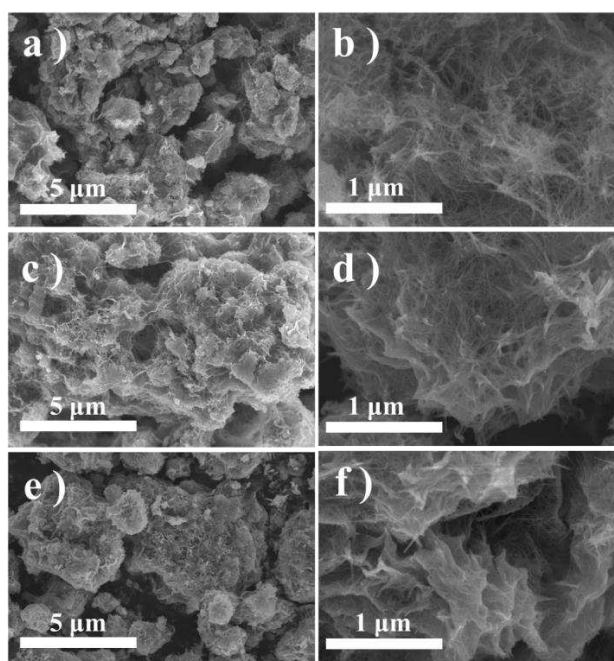
240 Where c_0 (mg/L) is the concentration of initial Cd^{2+} concentration and c_e (mg/L) is
241 the equilibrium Cd^{2+} concentration, respectively, V (L) is the volume of the solution
242 and m (g) is the weight of sorbent.

243

244 3 Results and discussions

245 3.1 Characterization

246 Figure 2 shows the SEM images of three adsorbents (TNT, TNT/C, TNT/HC). The
247 samples all showed some aggregation. In order to prove that these bundles or clusters
248 of material structures are nanotubes rather than nanowires, TEM was used for further
249 characterization.



250

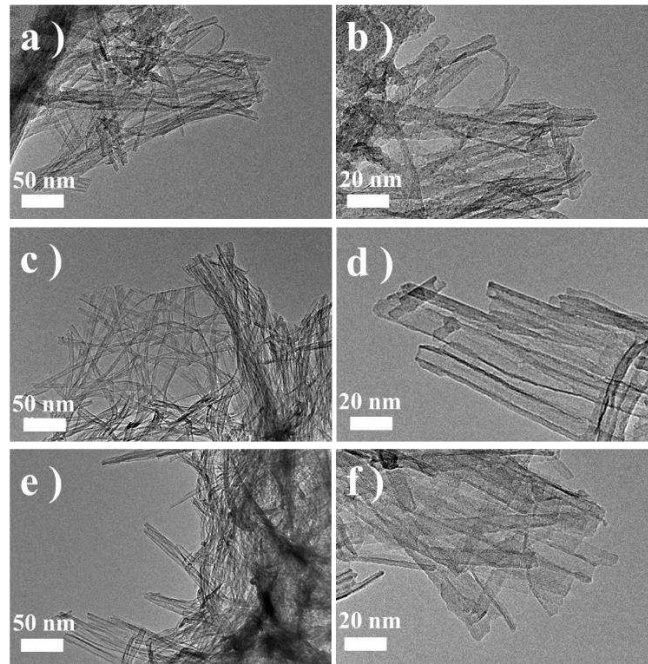
251

252 Fig. 2. SEM images of TNT (a, b), TNT@C (c, d) and TNT@HC (e, f)

253

254 Figure 3 demonstrates a typical TEM image of titanate nanotubes, which are
255 approximately 5-10 nm in diameter. Figure 4.a. shows the XRD patterns of the TNT,
256 TNT/C and TNT/HC. It is assumed that the peaks at the center of 10° , 24.3° , 28.5° and
257 48.2° are their characteristic diffraction peaks, which indicates that the synthesized
258 titanate nanotubes have the chemical formula of $\text{Na}_x\text{H}_{2-x}\text{Ti}_3\text{O}_7$ (Duan et al. 2021). The
259 peak at 10° is an indication of the interlayer distance of titanate (Zhao et al. 2016). The
260 SEM/TEM images and XRD patterns of TNT, TNT/C and TNT/HC are similar, which

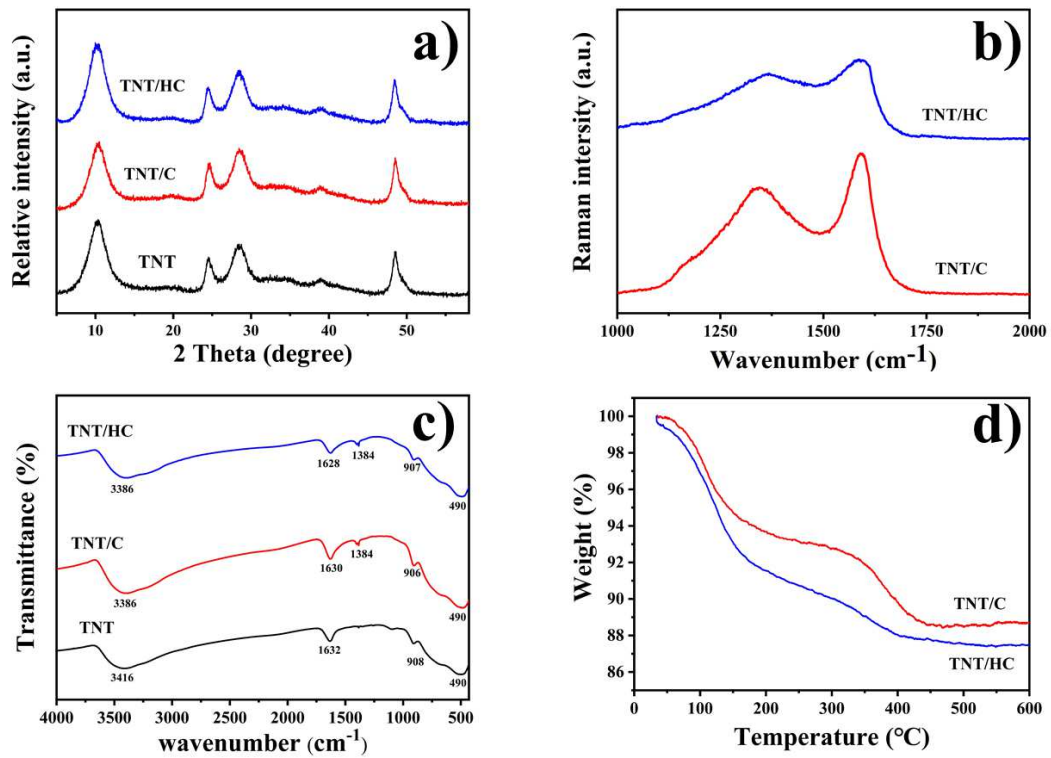
261 means that carbon loading on the TiO₂ surface does not affect the growth of TNT.



262

263

Fig.3. TEM images of TNT (a, b), TNT/C (c, d) and TNT/HC (e, f)



264

265 Fig. 4. Characterizations of the TNT, TNT/C and TNT/HC. (a) XRD pattern, (b)

266

Raman spectra, (c) FT-IR spectra, (d) Thermogravimetric profiles.

267

The Raman spectra of TNT/C and TNT/HC are shown in Figure 4.b. The two

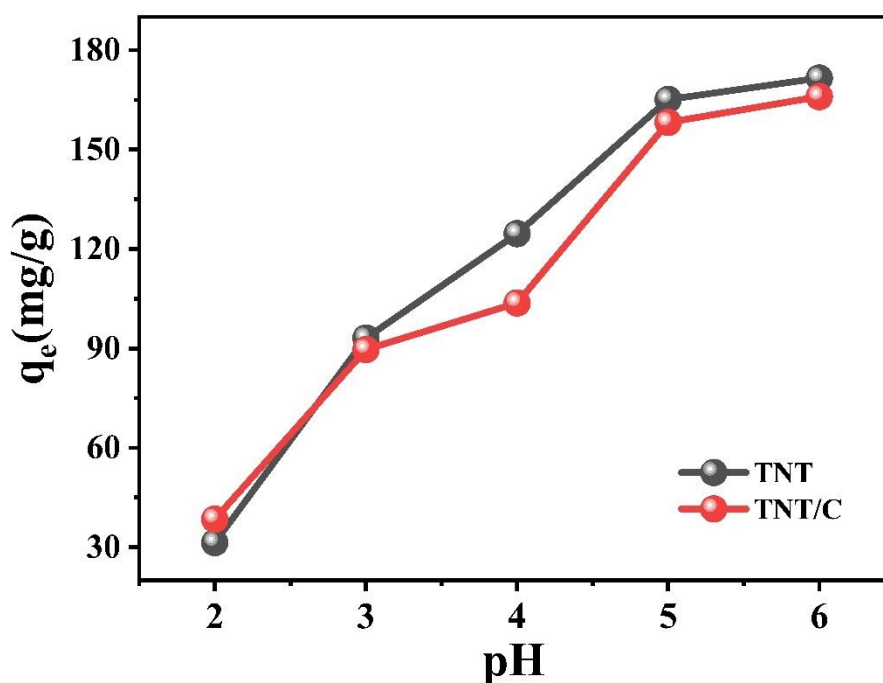
268 peaks at 1358 cm^{-1} and 1600 cm^{-1} correspond to the G peak and D peak of carbon,
269 which indicates the successful introduction of carbon (Pyrzyńska & Bystrzejewski
270 2010). The I_D/I_G TNT/HC (0.884) exceeding I_D/I_G TNT/C (0.806) indicates that the degree
271 of non-graphitization of TNT/HC is greater than that of TNT/C, which is caused by
272 nitric acid treatment. The FT-IR spectra of TNT, TNT/C and TNT/HC are given in
273 Figure 4.c. For the neat TNT, the strong absorption bands in the region of 3416 cm^{-1}
274 and the band at 1632 cm^{-1} could be attributed to the hydroxyl groups stretching
275 vibration and water molecules binding vibration, respectively, indicating the presence
276 of hydroxyl groups and water molecules in the TNT (Wang et al. 2018, Zhu et al. 2018).
277 The band at 908 cm^{-1} might be related to a four-coordinate Ti–O stretching vibration
278 (Wang et al. 2013b). The band at 490 cm^{-1} was assigned to the vibration of $[\text{TiO}_6]$
279 octahedron (Xiong et al. 2011). For TNT/C and TNT/HC, the new peak at 1384 cm^{-1} is
280 the carbonyl vibrations of ketone groups peak (Wang et al. 2013a). The
281 thermogravimetric profiles of TNT/C and TNT/HC could be seen in Figure 4.d. The
282 weight loss at temperatures below 100°C is due to the evaporation of free water on the
283 surface of the adsorbent (Yuan et al. 2017, Zhou et al. 2020). The weight loss at $100-$
284 350°C is attributed to the loss of chemically bonded water of the crystal layer. The
285 weight loss after 350°C is due to the oxidation of carbon. TNT/HC has no obvious
286 plateau at $200-350^\circ\text{C}$, which is caused by the superposition of the loss of chemically
287 bonded water in the crystal layer and the loss of carbon oxidation (Yuan et al. 2017).

288

289 3.2 Effects of pH

290 The pH value of the experimental solution has a great influence on the adsorption
291 results. According to previous studies, in order to avoid precipitation of Cd^{2+} hydroxide,
292 it was decided to choose an initial solution with a pH of 2-6 for exploration (Kim et al.
293 2020). The experimental results are shown in Figure 5. The adsorption capacity of TNT
294 and TNT/C for Cd^{2+} changes with the change of pH, and the relationship between them
295 is positively correlated. The maximum adsorption capacity occurs when the pH is 6.

296 Whether the adsorption mechanism is ion exchange or surface action, the adsorption of
297 positively charged Cd^{2+} and positively charged H^+ on the surface of the adsorbent is in
298 a competitive relationship. Therefore, when the pH is lower, the concentration of
299 hydrogen ions is also higher, and the competition between hydrogen ions and Cd^{2+} is
300 quite fierce. As we all know, pH is the negative logarithm of hydrogen ion. Because an
301 increase in the pH value by one value could cause the hydrogen ion concentration to
302 drop by an order of magnitude, so at the same time the ratio of Cd^{2+} to H^+ concentration
303 would increase. So, the adsorption capacity gradually increases with the increase of pH.



304

305 Fig. 5. Effect of initial pH on adsorption capacity of TNT and TNT/C.

306

307 3.3 Effects of contact time and adsorption kinetic

308 Figure 6.a shows the kinetics of Cd^{2+} adsorption on the TNT, TNT/C at 25 °C and
309 pH=6. Obviously, the adsorption capacity increases with the prolongation of the contact
310 time, and the adsorption equilibrium is reached within 150 minutes. The Cd^{2+}
311 absorption amounts of TNT, TNT/C are $171.56 \text{ mg}\cdot\text{g}^{-1}$ and $166 \text{ mg}\cdot\text{g}^{-1}$. Kinetic studies
312 have profound guiding significance for the explanation of the experimental mechanism

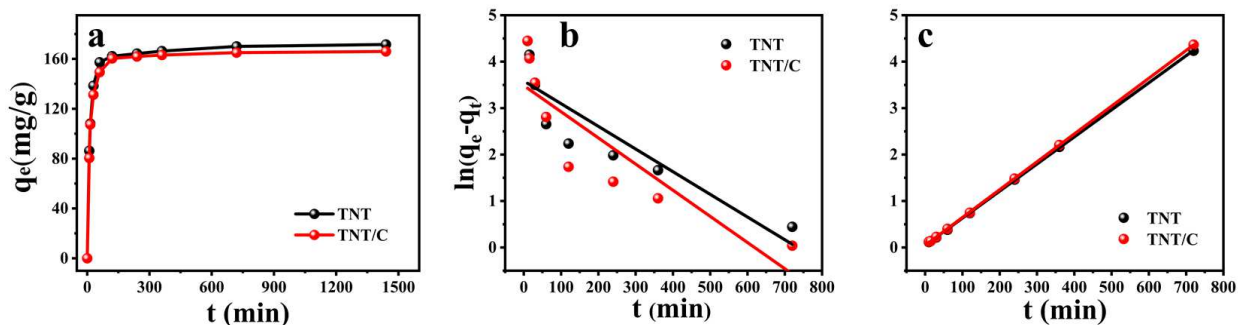
313 and the selection of the best adsorption time for the adsorbent. There are two commonly
 314 used semi-empirical models, namely pseudo-first-order (PFO) dynamics and pseudo-
 315 second-order (PSO) dynamics (Dalvand et al. 2018, Dolatyari et al. 2016). The pseudo
 316 first order dynamics is as follows□

$$317 \ln(q_e - q_t) = \ln q_e - k_1 * t \quad (2)$$

318 Where k_1 is the rate constant of pseudo-first-order adsorption, q_e (mg/g) and q_t (mg/g)
 319 is the amount of Cd^{2+} adsorbed at equilibrium and at time (t) (Goyal et al. 2020). The
 320 pseudo first order dynamics is as follows□

$$321 t/q_t = 1/(k_2 * q_e^2) + t/q_e \quad (3)$$

322 Where k_2 is the rate constant of pseudo-second-order adsorption (Rahman et al. 2020).
 323 The corresponding kinetic parameters are shown in Table 1. The pseudo -first-order
 324 kinetics and pseudo-second kinetics determination coefficient (R^2) of TNT/C are
 325 0.7623 and 0.9999. Similarly, the value of TNT/HC are 0.7396 and 0.9999. This
 326 indicates that pseudo-second-order kinetics is more suitable for the process of Cd^{2+}
 327 adsorption by TNT and TNT/C. Since the PSO model assumes that the chemical surface
 328 reaction is the rate-limiting step (Zhao et al. 2020), we concluded that the rate-
 329 determining step of Cd^{2+} adsorption on TNT and TNT/C was chemisorption (Zheng et
 330 al. 2021).



331
 332 Fig. 6. Adsorption kinetics (a), the Pseudo-first-order model(b) and the Pseudo-
 333 second-order model fitting curve of Cd^{2+} on TNT and TNT/C (c).

334 Table 1

335 Pseudo-first-order and pseudo-second-order parameters for adsorption of Cd^{2+} by TNT

Sample	pseudo-first-order kinetic				pseudo-second-order kinetic		
	$q_{e,exp}$ (mg/g)	$q_{e,cal}$ (mg/g)	k_1 (min ⁻¹)	R^2	$q_{e,cal}$ (mg/g)	k_2 (g/(mg*min))	R^2
TNT	171.56	36.0313	0.0049	0.7623	171.5266	0.4066	0.9999
TNT/C	166	32.6329	0.0056	0.7396	16.9449	0.3738	0.9999

337

338 3.4 Adsorption isotherms.

339 For the design and operation of adsorption systems, the correlation of equilibrium
 340 adsorption data is important. Langmuir and Freundlich isotherms models were applied
 341 to fit the obtained adsorption data (Wang et al. 2020). The Langmuir equation has been
 342 used extensively for dilute solutions in the following form:

$$343 \quad q_e = (q_m * K_L * c_e) / (1 + K_L * c_e) \quad (4)$$

344 Where c_e (mg·L⁻¹) is the equilibrium concentration of Cd²⁺ remained in solution,
 345 q_e (mg·g⁻¹) is the amount of solution adsorbed per unit mass of the adsorbent, q_m
 346 (mg·g⁻¹) is the maximum adsorption capacity, K_L is the Langmuir adsorption
 347 equilibrium constant (Tang et al. 2020). The Freundlich equation has been used
 348 extensively for dilute solutions in the following form:

$$349 \quad \ln q_e = \ln K_F + 1/n * \ln c_e \quad (5)$$

350 Where K_F and n are the Freundlich constants related to the adsorption capacity
 351 and adsorption intensity, respectively (Mao et al. 2018). The curve of the adsorption
 352 isotherm model and the fitting data are shown in Figure 7 and Table 2. The results show
 353 the Langmuir isotherm model better fits the experimental results with high correlation
 354 coefficients (>0.97). The Langmuir model indicates that it is monolayer adsorption on
 355 the structurally homogeneous TNT and TNT/C.

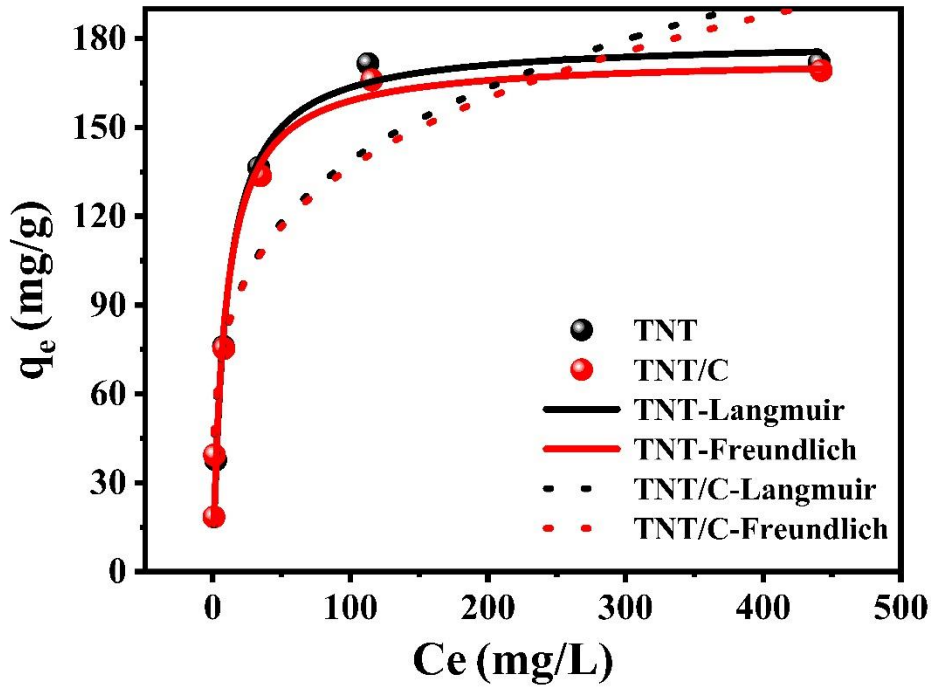


Fig. 7. Adsorption isotherm of Cd^{2+} on TNT and TNT/C

356

357

358

359 Table 2

360 Parameters of Langmuir and Freundlich isotherm models for the adsorption of Cd^{2+} on

361 TNT, TNT@C.

Samples	Langmuir equation			Freundlich equation		
	q_m mg/g	K_L L/mg	R^2	K_F	$\frac{1}{n}$	R^2
TNT	179.37	0.1026	0.9951	47.0877	4.2597	0.8119
TNT/C	173.31	0.1109	0.9806	47.5353	4.3662	0.8375

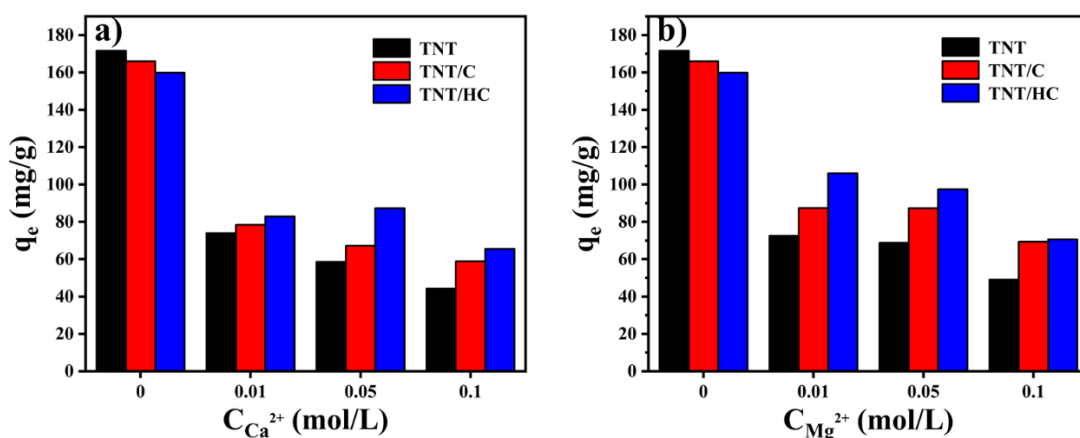
362

363 3.5 Effects of ionic strength (Ca^{2+} , Mg^{2+})

364 Figure 8 shows the competition between coexisting cations and Cd^{2+} on TNT,

365 TNT/C and TNT/HC. Generally, the adsorption capacity of Cd^{2+} will decrease in the

366 presence of Ca^{2+} or Mg^{2+} (Liu et al. 2013). This is due to the competition adsorption
 367 between Ca^{2+} or Mg^{2+} and Cd^{2+} . In this paper, the adsorption capacity of Cd^{2+} also
 368 decreases when Ca^{2+} or Mg^{2+} exists in the adsorption environment, but the adsorption
 369 capacity of TNT/C and TNT/HC exceeds that of Cd^{2+} absorbed by TNT due to the
 370 loading of carbon. When Ca^{2+} or Mg^{2+} exists in the adsorption environment, the order
 371 of the adsorption capacity of Cd^{2+} to different adsorption materials is
 372 TNT/HC>TNT/C>TNT. But the order of adsorption capacity is
 373 TNT>TNT/C>TNT/HC in the absence of Ca^{2+} or Mg^{2+} . It is also interesting to see that
 374 the anti-interference ability of TNT/HC prepared by hydrothermal method is improved
 375 after the carbon on the surface of TiO_2 is oxidized by nitric acid (TNT/HC). The
 376 experimental results also show that when the concentration of Ca^{2+} or Mg^{2+} is high up
 377 to 0.1 mol/L, the adsorption capacity of TNT/HC on Cd^{2+} increases from 44.28 mg/L
 378 to 65.52 mg/L (in the presence of Ca^{2+}), and from 49.04 mg/L to 66.6 mg/L (in the
 379 presence of Mg^{2+}) compared with TNT. It is proved that TNT/HC is more promising
 380 than TNT as an adsorbent for the selective separation of Cd^{2+} from complex water
 381 conditions.

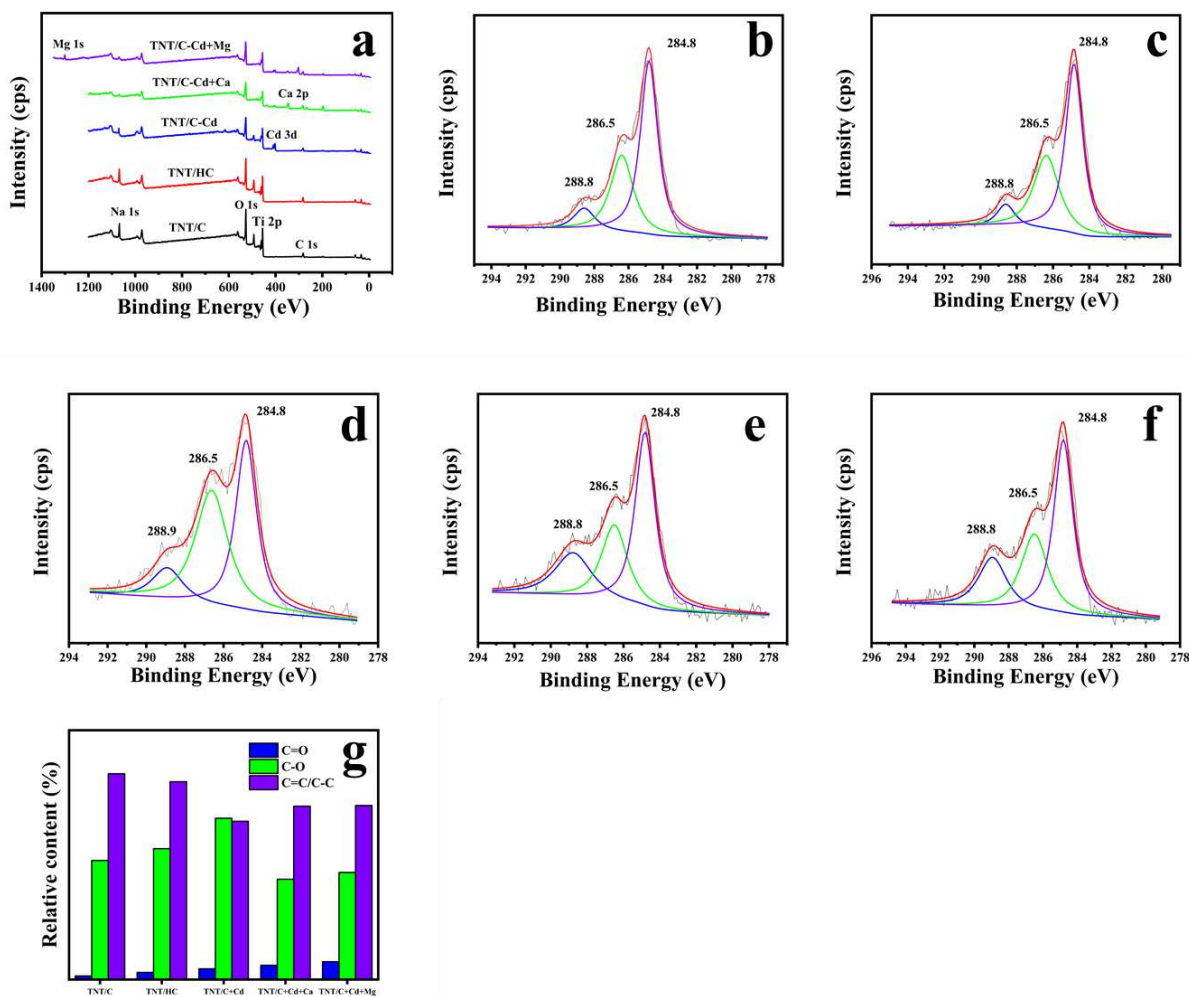


382
 383 Fig. 8. The adsorption capacity of Cd^{2+} on TNTs, TNTs/C and TNTs/HC with or
 384 without the presence of Ca^{2+} (a) or Mg^{2+} (b).

385

386 3.6 Mechanisms of competitive adsorption

387 In order to reveal the competitive adsorption mechanism of TNT based adsorbents to
388 metal ions, we tested the XPS spectra of adsorbents before and after adsorption. The
389 experimental results are shown in the figure 9. In the wide-scan spectrum, after the
390 adsorption of Cd^{2+} , Ca^{2+} , and Mg^{2+} , the peaks of sodium ions almost disappeared, and
391 Cd^{2+} , Ca^{2+} , and Mg^{2+} peaks appeared, which indicates that the adsorption of Cd^{2+} , Ca^{2+} ,
392 and Mg^{2+} are achieved (Huang et al. 2020b). This reveals that the main adsorption
393 mechanism is the sodium ion exchange with metal ions in the TNT layers. In the narrow
394 sweep of C 1s, the peaks at 284.8, 286.5, and 288.8 eV represent C=C/C-C, C-O, and
395 C=O, respectively (Yang et al. 2020). After the adsorption of Cd^{2+} , the C=C/C-C peak
396 decreased (from 57.79% to 44.45%). This indicates that the cadmium ion-*p* effect
397 supports the loading of Cd^{2+} on C. In the $\text{Cd}^{2+}+\text{Ca}^{2+}$ and $\text{Cd}^{2+}+\text{Mg}^{2+}$ systems, the C=C
398 and C-O peak decreases after adsorption (Yuan et al. 2020). This can be explained by
399 the theory of hard and soft acids and bases: Ca^{2+} and Mg^{2+} belong to the ranks of hard
400 acids and C-O belongs to hard base, while Cd^{2+} is classified as soft acid. it is caused by
401 the complexation of C-O to Ca^{2+} and Mg^{2+} , while C-O is not interested in Cd^{2+} . This is
402 why the adsorption capacity of TNT/C is greater than that of neat TNT. And the
403 experimental data shows that there is Ca^{2+} or Mg^{2+} in the water, the order of Cd^{2+}
404 adsorption is TNT/HC>TNT/C>TNT, which is consistent with the order of C-O content.



405

406

407 Fig. 9. XPS wide-scan spectra (a); C1s XPS spectra off TNT/C(b), TNT/HC(c),

408 TNT/HC-Cd(d), TNT/C-Cd +Ca(e) and TNT/C-Cd +Mg(f); (g) the content of carbon-

409

410 4. Conclusions

411 We successfully synthesized titanate nanotubes and compounded a layer of carbon

412 on the surface of titanate nanotubes in situ. A series of characterization of the

413 synthesized adsorbent were carried by SEM, TEM and XRD. The characterization

414 results show that the modification of carbon does not affect the formation of titanate

415 nanotubes. Through experiments, we have obtained the optimal pH value for Cd²⁺

416 adsorption by TNT and TNT/C which is pH=6; the pseudo-second-order kinetic model

417 and Langmuir isotherm adsorption model are more suitable for the adsorption process,
418 which means chemical adsorption and single-layer adsorption occurs during the
419 adsorption of Cd^{2+} on TNT and TNT/C. However, the fact that Ca^{2+} and Mg^{2+} inhibit
420 the adsorption of Cd^{2+} on titanate nanotubes is well known. We set out to solve this
421 problem by loading a layer of carbon in situ on the surface of TNT and then activating
422 it with strong acid. Experimental results show that this procedure improved the
423 competitive adsorption of Cd^{2+} in the presence of Ca^{2+} or Mg^{2+} . Although the surface
424 loading of a layer of carbon lowers the total adsorption capacity of titanate nanotubes
425 for ions (the order of adsorption capacity is $\text{TNT} > \text{TNT/C} > \text{TNT/HC}$ in the absence of
426 Ca^{2+} or Mg^{2+}), it improves its ability of resist interference from Ca^{2+} and Mg^{2+} (the
427 order of adsorption capacity of Cd^{2+} on different adsorption materials is
428 $\text{TNT/HC} > \text{TNT/C} > \text{TNT}$ in the presence of Ca^{2+} or Mg^{2+}). Although it is not the first
429 time to pay attention to the influence of Ca^{2+} and Mg^{2+} on titanate nanotube adsorbent,
430 as far as we know, this is the first time to try to solve this problem and get a positive
431 response. This paper provides an idea for the research and development of heavy metal
432 ion adsorbents.

433 **Declarations**

434 **Ethics approval and consent to participate:** Not applicable.

435 **Consent for publication:** Not applicable.

436 **Availability of data and materials:** All data generated or analysed during this study
437 are included in this published article.

438 **Conflicts of interest:** The authors declare no conflict of interest.

439 **Funding:** This research received no external funding.

440 **Author Contributions:** This research was designed, implemented and written by Mr.
441 Mingda Wu; the research was supervised by Ms. Tao Zhou. Mr. Yi Ma and Zhengsong
442 Weng performed statistical analysis, Professor Linghong Lu provided laboratory
443 support.

444 **Acknowledgements:** The project gets the funding support from the National Natural

445 Science Foundation of China (NO.21676137 and NO.21838004).

446 References

- 447 Bi J, Huang X, Wang J, Tao Q, Wang T, Hao H (2020): Titanate for water remediation:
448 synthesis, application, mechanism and optimization. *Journal of Materials*
449 *Chemistry A* 8, 14415-14440
- 450 Bolisetty S, Peydayesh M, Mezzenga R (2019): Sustainable technologies for water
451 purification from heavy metals: review and analysis. *Chem Soc Rev* 48, 463-
452 487
- 453 Boparai HK, Joseph M, O'Carroll DM (2011): Kinetics and thermodynamics of cadmium
454 ion removal by adsorption onto nano zerovalent iron particles. *J Hazard Mater*
455 186, 458-65
- 456 Dalvand A, Khoobi M, Nabizadeh R, Ganjali MR, Gholibegloo E, Mahvi AH (2018): Reactive
457 Dye Adsorption from Aqueous Solution on HPEI-Modified Fe₃O₄ Nanoparticle as
458 a Superadsorbent: Characterization, Modeling, and Optimization. *Journal of*
459 *Polymers and the Environment* 26, 3470-3483
- 460 Di Natale F, Gargiulo V, Alfe M (2020): Adsorption of heavy metals on silica-supported
461 hydrophilic carbonaceous nanoparticles (SHNPs). *J Hazard Mater* 393, 122374
- 462 Dolatyari L, Yaftian MR, Rostamnia S (2016): Removal of uranium(VI) ions from aqueous
463 solutions using Schiff base functionalized SBA-15 mesoporous silica materials.
464 *J Environ Manage* 169, 8-17
- 465 Du AJ, Sun DD, Leckie JO (2011): Sequestration of cadmium ions using titanate nanotube.
466 *J Hazard Mater* 187, 401-6
- 467 Duan J, Ji H, Xu T, Pan F, Liu X, Liu W, Zhao D (2021): Simultaneous adsorption of
468 uranium(VI) and 2-chlorophenol by activated carbon fiber supported/modified
469 titanate nanotubes (TNTs/ACF): Effectiveness and synergistic effects.
470 *Chemical Engineering Journal* 406
- 471 Esrafil L, Firuzabadi FD, Morsali A, Hu ML (2021): Reuse of Predesigned Dual-
472 Functional Metal Organic Frameworks (DF-MOFs) after Heavy Metal Removal. *J*
473 *Hazard Mater* 403, 123696
- 474 Goyal N, Gao P, Wang Z, Cheng S, Ok YS, Li G, Liu L (2020): Nanostructured
475 chitosan/molecular sieve-4A an emergent material for the synergistic
476 adsorption of radioactive major pollutants cesium and strontium. *J Hazard*
477 *Mater* 392, 122494
- 478 Huang K, Lv X, Guan X, Liu J, Li S, Song H (2020a): Advanced Cd (II) adsorbent
479 fabricated with hordein from barley (*Hordeum vulgare* L.) via electrospinning
480 technology. *Industrial Crops and Products* 152
- 481 Huang X, Zhao H, Hu X, Liu F, Wang L, Zhao X, Gao P, Ji P (2020b): Optimization of
482 preparation technology for modified coal fly ash and its adsorption properties
483 for Cd(2). *J Hazard Mater* 392, 122461
- 484 Kasuga T, Hiramatsu M, Hoson A, Sekino T, Niihara K (1998): Formation of titanium
485 oxide nanotube. *Langmuir* 14, 3160-3163

486 Kim D-W, Wee J-H, Yang C-M, Yang KS (2020): Efficient removals of Hg and Cd in
487 aqueous solution through NaOH-modified activated carbon fiber. *Chemical*
488 *Engineering Journal* 392

489 Li X, Liu W, Ni J (2015): Short-cut synthesis of tri-titanate nanotubes using nano-
490 anatase: Mechanism and application as an excellent adsorbent. *Microporous and*
491 *Mesoporous Materials* 213, 40-47

492 Liu W, Wang T, Borthwick AGL, Wang Y, Yin X, Li X, Ni J (2013): Adsorption of Pb²⁺,
493 Cd²⁺, Cu²⁺ and Cr³⁺ onto titanate nanotubes: Competition and effect of
494 inorganic ions. *Science of The Total Environment* 456-457, 171-180

495 Liu W, Sun W, Han Y, Ahmad M, Ni J (2014): Adsorption of Cu(II) and Cd(II) on titanate
496 nanomaterials synthesized via hydrothermal method under different NaOH
497 concentrations: Role of sodium content. *Colloids and Surfaces A:*
498 *Physicochemical and Engineering Aspects* 452, 138-147

499 Lu F, Astruc D (2018): Nanomaterials for removal of toxic elements from water.
500 *Coordination Chemistry Reviews* 356, 147-164

501 Ma J, Li F, Qian T, Liu H, Liu W, Zhao D (2017): Natural organic matter resistant
502 powder activated charcoal supported titanate nanotubes for adsorption of
503 Pb(II). *Chemical Engineering Journal* 315, 191-200

504 Mahdavi S, Jalali M, Afkhami A (2013): HEAVY METALS REMOVAL FROM AQUEOUS SOLUTIONS
505 USING TiO₂, MgO, AND Al₂O₃ NANOPARTICLES. *Chemical Engineering Communications*
506 200, 448-470

507 Mao X, Wang L, Gu S, Duan Y, Zhu Y, Wang C, Lichtfouse E (2018): Synthesis of a
508 three-dimensional network sodium alginate - poly(acrylic acid)/attapulgite
509 hydrogel with good mechanic property and reusability for efficient adsorption
510 of Cu²⁺ and Pb²⁺. *Environmental Chemistry Letters* 16, 653-658

511 Maroto-Valer MM, Dranca I, Lupascu T, Nastas R (2004): Effect of adsorbate polarity
512 on thermodesorption profiles from oxidized and metal-impregnated activated
513 carbons. *Carbon* 42, 2655-2659

514 Mudhoo A, Ramasamy DL, Bhatnagar A, Usman M, Sillanpaa M (2020): An analysis of the
515 versatility and effectiveness of composts for sequestering heavy metal ions,
516 dyes and xenobiotics from soils and aqueous milieus. *Ecotoxicol Environ Saf*
517 197, 110587

518 Pyrzyńska K, Bystrzejewski M (2010): Comparative study of heavy metal ions sorption
519 onto activated carbon, carbon nanotubes, and carbon-encapsulated magnetic
520 nanoparticles. *Colloids and Surfaces A: Physicochemical and Engineering*
521 *Aspects* 362, 102-109

522 Rahman ML, Fui CJ, Sarjadi MS, Arshad SE, Musta B, Abdullah MH, Sarkar SM, O'Reilly
523 EJ (2020): Poly(amidoxime) ligand derived from waste palm fiber for the
524 removal of heavy metals from electroplating wastewater. *Environ Sci Pollut*
525 *Res Int*

526 Sriram G, Kigga M, Uthappa UT, Rego RM, Thendral V, Kumeria T, Jung HY, Kurkuri MD
527 (2020): Naturally available diatomite and their surface modification for the

528 removal of hazardous dye and metal ions: A review. *Adv Colloid Interface Sci*
529 282, 102198

530 Tang C, Brodie P, Li Y, Grishkewich NJ, Brunsting M, Tam KC (2020): Shape recoverable
531 and mechanically robust cellulose aerogel beads for efficient removal of
532 copper ions. *Chemical Engineering Journal* 392

533 Wang Q, Lei X, Pan F, Xia D, Shang Y, Sun W, Liu W (2018): A new type of activated
534 carbon fibre supported titanate nanotubes for high-capacity adsorption and
535 degradation of methylene blue. *Colloids and Surfaces A: Physicochemical and*
536 *Engineering Aspects* 555, 605-614

537 Wang R, Chen H, Xiao Y, Hadar I, Bu K, Zhang X, Pan J, Gu Y, Guo Z, Huang F,
538 Kanatzidis MG (2019): $K_x[Bi_{4-x}Mn_xS_6]$, Design of a Highly Selective Ion
539 Exchange Material and Direct Gap 2D Semiconductor. *J Am Chem Soc* 141, 16903-
540 16914

541 Wang T, Liu W, Xiong L, Xu N, Ni J (2013a): Influence of pH, ionic strength and humic
542 acid on competitive adsorption of Pb(II), Cd(II) and Cr(III) onto titanate
543 nanotubes. *Chemical Engineering Journal* 215-216, 366-374

544 Wang T, Liu W, Xu N, Ni J (2013b): Adsorption and desorption of Cd(II) onto titanate
545 nanotubes and efficient regeneration of tubular structures. *Journal of*
546 *Hazardous Materials* 250-251, 379-386

547 Wang Z, Wu S, Zhang Y, Miao L, Zhang Y, Wu A (2020): Preparation of modified sodium
548 alginate aerogel and its application in removing lead and cadmium ions in
549 wastewater. *Int J Biol Macromol* 157, 687-694

550 Xiong L, Chen C, Chen Q, Ni J (2011): Adsorption of Pb(II) and Cd(II) from aqueous
551 solutions using titanate nanotubes prepared via hydrothermal method. *J Hazard*
552 *Mater* 189, 741-8

553 Yang X, Guo N, Yu Y, Li H, Xia H, Yu H (2020): Synthesis of magnetic graphene oxide-
554 titanate composites for efficient removal of Pb(II) from wastewater:
555 Performance and mechanism. *Journal of Environmental Management* 256

556 Yuan F, Wu C, Cai Y, Zhang L, Wang J, Chen L, Wang X, Yang S, Wang S (2017): Synthesis
557 of phytic acid-decorated titanate nanotubes for high efficient and high
558 selective removal of U(VI). *Chemical Engineering Journal* 322, 353-365

559 Yuan S, Hong M, Li H, Ye Z, Gong H, Zhang J, Huang Q, Tan Z (2020): Contributions
560 and mechanisms of components in modified biochar to adsorb cadmium in aqueous
561 solution. *Sci Total Environ* 733, 139320

562 Yusuf M, Song K, Geng S, Fazhi X (2020): Adsorptive removal of anionic dyes by
563 graphene impregnated with MnO₂ from aqueous solution. *Colloids and Surfaces*
564 *A: Physicochemical and Engineering Aspects* 595

565 Zhang J, Hou D, Shen Z, Jin F, O'Connor D, Pan S, Ok YS, Tsang DCW, Bolan NS, Alessi
566 DS (2020): Effects of excessive impregnation, magnesium content, and pyrolysis
567 temperature on MgO-coated watermelon rind biochar and its lead removal
568 capacity. *Environmental Research* 183

569 Zhang S, Cui M, Chen J, Ding Z, Wang X, Mu Y, Meng C (2019): Modification of synthetic

570 zeolite X by thiourea and its adsorption for Cd (II). *Materials Letters* 236,
571 233-235

572 Zhao F, Yang Z, Wei Z, Spinney R, Sillanpää M, Tang J, Tam M, Xiao R (2020):
573 Polyethylenimine-modified chitosan materials for the recovery of La(III) from
574 leachates of bauxite residue. *Chemical Engineering Journal* 388

575 Zhao G, Li J, Ren X, Chen C, Wang X (2011): Few-layered graphene oxide nanosheets as
576 superior sorbents for heavy metal ion pollution management. *Environ Sci*
577 *Technol* 45, 10454-62

578 Zhao X, Cai Z, Wang T, O' Reilly SE, Liu W, Zhao D (2016): A new type of cobalt-
579 deposited titanate nanotubes for enhanced photocatalytic degradation of
580 phenanthrene. *Applied Catalysis B: Environmental* 187, 134-143

581 Zheng C, Wu Q, Hu X, Wang Y, Chen Y, Zhang S, Zheng H (2021): Adsorption behavior of
582 heavy metal ions on a polymer-immobilized amphoteric biosorbent: Surface
583 interaction assessment. *Journal of Hazardous Materials* 403

584 Zhou G, Luo J, Liu C, Chu L, Crittenden J (2018): Efficient heavy metal removal from
585 industrial melting effluent using fixed-bed process based on porous hydrogel
586 adsorbents. *Water Res* 131, 246-254

587 Zhou Y, Li Y, Liu D, Wang X, Liu D, Xu L (2020): Synthesis of the inorganic-organic
588 hybrid of two-dimensional polydopamine-functionalized titanate nanosheets and
589 its efficient extraction of U(VI) from aqueous solution. *Colloids and Surfaces*
590 *A: Physicochemical and Engineering Aspects* 607

591 Zhu J, Liu Q, Li Z, Liu J, Zhang H, Li R, Wang J (2018): Efficient extraction of
592 uranium from aqueous solution using an amino-functionalized magnetic titanate
593 nanotubes. *J Hazard Mater* 353, 9-17

594